Plant moisture measurement in field trials based on NIR spectral imaging – a feasibility study

Marius Thiel[1], Thomas Rath[2], Arno Ruckelshausen[1]
[1] University of Applied Sciences Osnabrück/ Faculty of Engineering and Computer Science
Albrechtstr. 30, 49076 Osnabrück, Germany, ma.thiel@fh-osnabrueck.de
[2] Leibniz University Hannover/ Institute for Bioproduction Systems
Herrenhäuser Str. 2, 30419 Hannover, Germany

ABSTRACT

This paper deals with a feasibility study of a near-infrared spectral imaging system related to its ability for in-situ plant moisture measurements in agricultural environments. First the influences of water to the spectral characteristic of leafs is shown and a basic water index was correlated to moisture. Using an active illumination the spatial and spectral resolution of a NIR spectral imaging system for plant characterization has been evaluated. Also environmental and plant influences as well as data management aspects are figured out. Moreover a first dynamic test for moisture measurement using a powered conveyor system has been performed. Based on this study conclusions are presented for automated plant rating based on NIR imaging.

Keywords: Spectral imaging, spectral reflectance, near-infrared, plant moisture measurement, precision agriculture, plant phenotyping, plant breeding process, Germany

1. INTRODUCTION

Measuring plant properties is of high importance for field trials in agriculture. Especially in the field of plant breeding the rating process takes a key role and is applied to every operation step (Thomas 2006). Till now the data acquisition of plant conditions is mainly performed manually by experts considering random samples of single plants or parts of field plots - this results in a statistical overview of the total field (Walter et al. 2000). In addition to statistical inaccuracies the comparability of these results becomes more difficulty caused by varying experts (Dicke 2005).

Using sensor technology gives the potential to automate the characterization of plants. Thus there is a potential to analyze each single plant in a complete objective way (Ruckelshausen et al. 2009). Next to other technologies spectral sensors are able to detect several important characteristics of plants. In addition to photosynthesis activity further plant conditions e.g. moisture can be analyzed by measuring the electromagnetic reflectance (Groell et al. 2006, Hellebrand et al. 2005, Larsole 2007). Moreover the spatial resolution of spectral imaging offers the advantage to combine spectral analysis with image processing. Using this technology under laboratory conditions the moisture dispersion of a single leaf has been measured and visualized (Smolyar 2003). Moisture dispersion of plants can be used as an indicator e.g. of plant stress situations or plant diseases causes variances of water concentration from plant to plant or within single leafs.

The next step is to use the technology of spectral imaging for measuring leaf characteristics of complete plants on fields. To apply this technology for in-situ plant ratings e.g. in breeding procedures the sensor system characteristic as well as disturbances of the environment which influences the spectral reflectance have to be identified and analyzed. Based on this analysis

M. Thiel, T. Rath, A. Ruckelshausen. “Plant moisture measurement in field trials based on NIR spectral imaging – a feasibility study” CIGR Workshop on Image Analysis in Agriculture, 26-27. August 2010, Budapest.

appropriate methods to compensate these influences have to be developed and evaluated. Moreover, the high data volume requires a corresponding system architecture.

2. MATERIALS AND METHODS

On the market many different sensor types are available to receive spectral data (table 1) – most of them are able to measure this data in combination with spatial information to generate a spectral cube with spatial 2D-data and the related spectral data of each single spatial pixel.

Table 1: Overview of different sensor components for spectral analyses

	Hardware	Typ. spectral resolution	Wavebands > 10	„Real-time“	VIS/NIR	Imaging system
	Programmable filter	10-20nm	X	-	X	X
	Miniature spectroscope	5nm	X	X	X	-
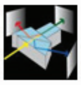	Multichip-Camera	10-20nm	-	X	X	X
	Spectral Imaging System	10nm	X	X	X	X

The advantage of the spectral imaging system is to generate the spectral information parallel with high count of available wavebands with a high spectral resolution of typical 10 nm FWHM (full width half mean) - dependence of the slit width. Therefore it gives a very high flexibility especially for research analyzing detailed reflectance spectra of objects. High frame rates additionally allow online measurements in contrast to the technology of programmable filter.

The sensor system used for the feasibility study was the Helios Core NIR from the company EVK DI Kerschhaggl GmbH, Austria.

Table 2: Datasheet summary (EVK)

Helios Core NIR	
Interface	Gigabit Ethernet
Sensor	InGaAs 320 x 256 pixel
Output data	252 pixel spectral 240 pixel spatial
Dynamic	12 Bit
Spectral range	0.9-1.7 µm
Slit width	100 µm
Frame rate	330 Hz full frame

Figure 1: EVK Helios Core [source: evk.biz]

This system consists of an imaging spectrograph, which expands the light with a specific optic into its spectral components of the NIR band from 0.9µm to 1.7µm. Thus the spectral information as well as line wise spatial information is given by a near-infrared camera which is also a main component of this system.

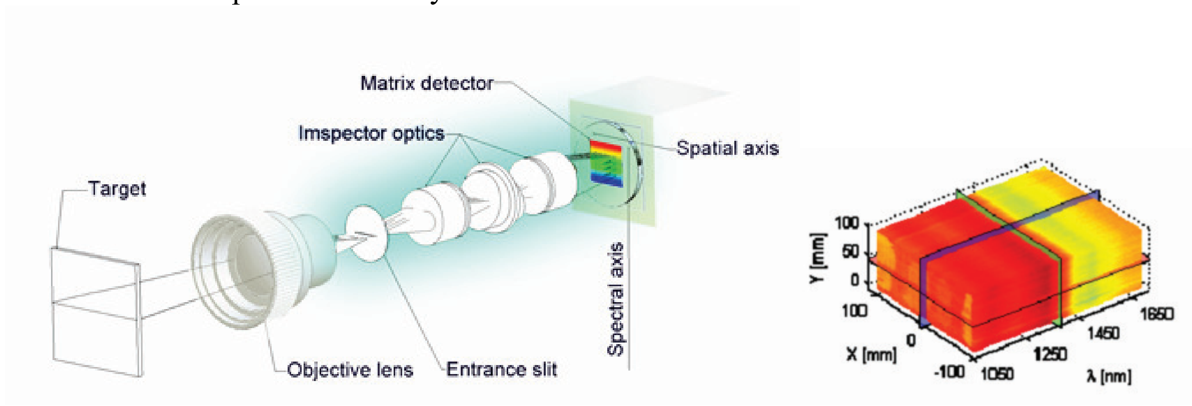

Figure 2: Schematic functional principle of the Spectral imaging sensor system (left) [source: specim.fi]; hyper spectral data cube (right) [source: EVK.biz]

For this feasibility study a special test setup was engineered to be able to confirm reproducible measurements. The test setup is equipped with a linear drive system powered by a stepper motor which is able to move a 600 mm x 600 mm designed ground plate on a linear path of 700 mm. The stepper motor allows high moving speed up to 1m/s as well as very tiny and slow moving steps. On the ground plate different object as well as whole plants and soil can be placed. This setup was be used to identify the system characteristics of the spectral imaging system and the relevant environmental influences for in-situ plant measurements.

Table 3: Datasheet of powered conveyor setup

Powered conveyor test setup	
Interface	USB
Drive system	Stepper / drive belt
Speed	0…1 ms^{-1}
Linear path	700 mm
Illumination	2 x Halogen 65W
Sensor height above ground plate	800 mm (adjustable)
Size of ground plate	600 mm x 600 mm
Lens	8 mm
Lens aperture	5,6

Figure 3: Powered conveyor test setup

The following system characteristics and environmental parameters which are of high importance for in-situ measurements are identified and described in this paper.

Table 4: measured characteristics of the sensor system and the environment

System characteristic
Spectral sensor calibration
Sensor line width
Spatial resolution
Spectral resolution
Signal to noise ratio

Environmental parameter
Plant moisture
Plant reflectance
Soil reflectance
Plant height

3. RESULTS AND DISCUSSION

To identify the most important system characteristics and environmental parameters of the spectral imaging setup different experimental measurements were performed.

2.1 Pilot survey: spectral characteristics of leaf and soil influenced by water

Two of the main well-known strong water absorbance bands in the near infrared < 2 µm are at the wavelength 1.46 µm and 1.94 µm. The following measurement performed with fiber optical spectroscopes (Ocean Optics S2000 / Tec5 PGS-NIR 2.2) shows the typical reflectance from 500 nm to 2100 nm of a fresh leaf as well as of a dried one of maize.

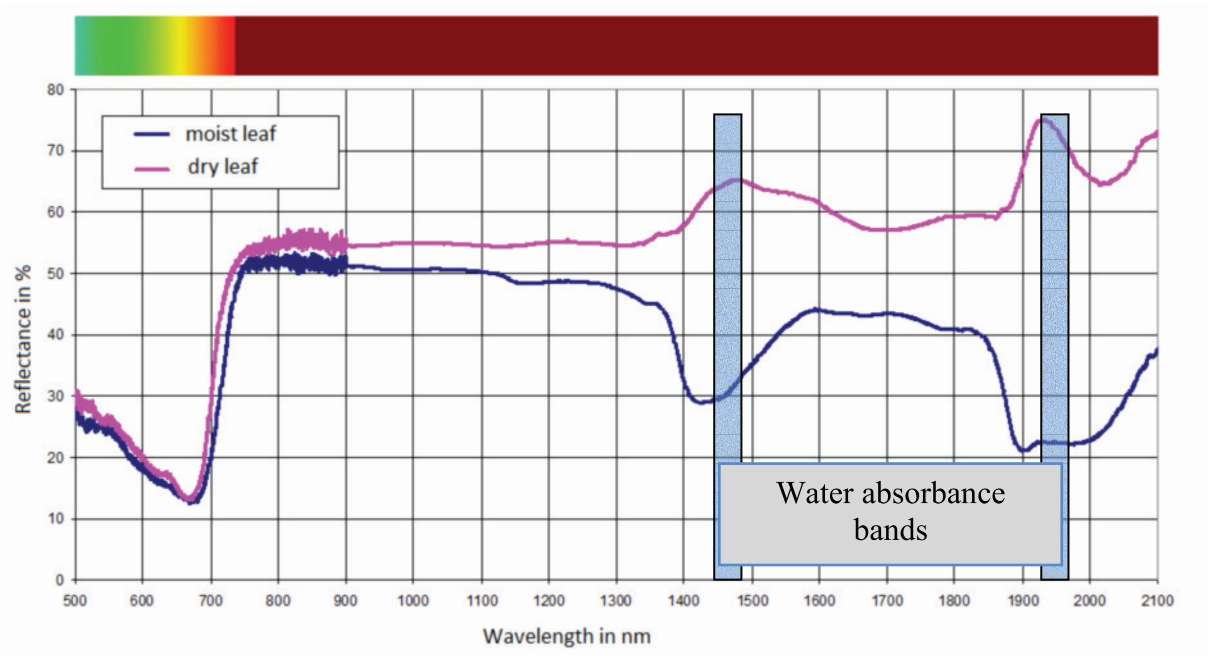

Figure 4: Typical reflectance of a moist and dried leaf with marked water absorption band in the near-infrared waveband

The influences of the spectral absorbance of water are clearly pointed out (Figure 4). In addition to regions with strong water dependency e.g. the region of 1.46 µm other regions with only minimal influences between 0.8 µm and 1.1 µm are identified. This fact is very important for being able to scale the reflectance data in case of different offset reflectance intensities e.g. based on variation of illumination intensities. A basic water index to qualify moisture of measured objects is established:

Water index: $WI = \frac{R_{1460}}{R_{1000}}$ | R_x: Reflectance at x nm wavelength

In addition to the range of leaf reflectance the signatures of soil with different level of humidity has been measured.

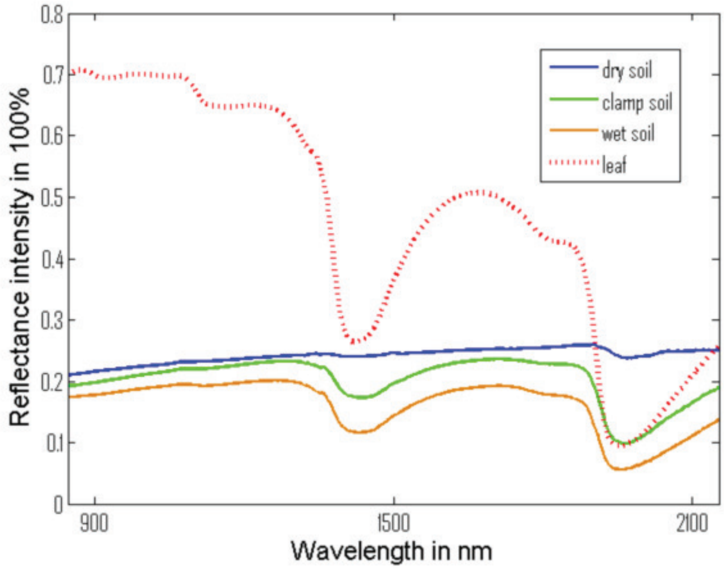

Figure 5: Typical reflectance intensity of soil with different level of humidity

As shown (Figure 5) the reflectance of soil overall is lower than the typical reflectance of a leaf in the working range of the Helios Core system (0.9 µm-1.7 µm). But also there is a strong dependency of water at 1.46 µm and 1.94 µm.
To validate the correlation of the water absorbance band 1.46µm and the moisture of objects small sponges were used and filled with different volume of liquid water. In contrast to real leafs sponges allow a wide range of moistures intensities with nearly homogeneous dispersion of water at the whole object.
The reflectance at the near-infrared band was measured with the Tec5 NIR-spectroscope. After measuring the sponges were dried out in a drying oven. Their primal moisture was determined by calculating the difference of moist mass and dry mass.

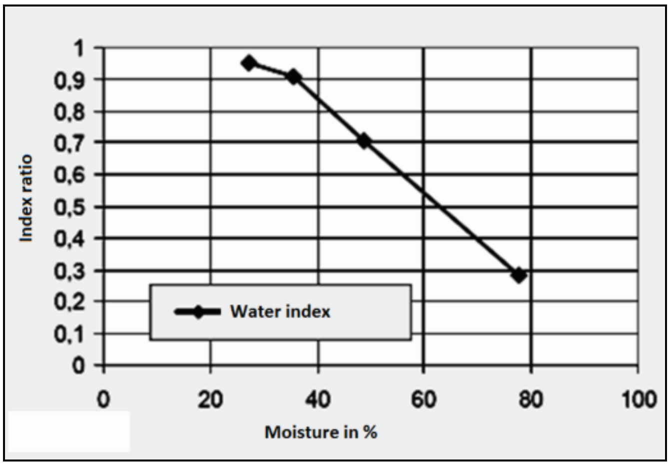

Figure 6: Setup for sponge moisture measuring (left); measured correlation of basic water index / moisture (right)

A clear correlation between the basic water index and the moisture of the sponges was pointed out. To be able to get precise spectral data with the used spectral imaging system the system has to be calibrated. Due to this the correlation between the spectral sensor pixel and its exact wavelength has to be measured.

2.2 Spectral calibration

For have a direct correlation between each spectral sensor pixel and its corresponding wavelengths the peak wavelengths of four different light emitting diodes were measured using the already precise calibrated Tec5-spectroscope. Similarly the field of view of the spectral imaging system was illuminated by these LEDs. Having a look to the raw data the corresponding intensity maxima were indentified.

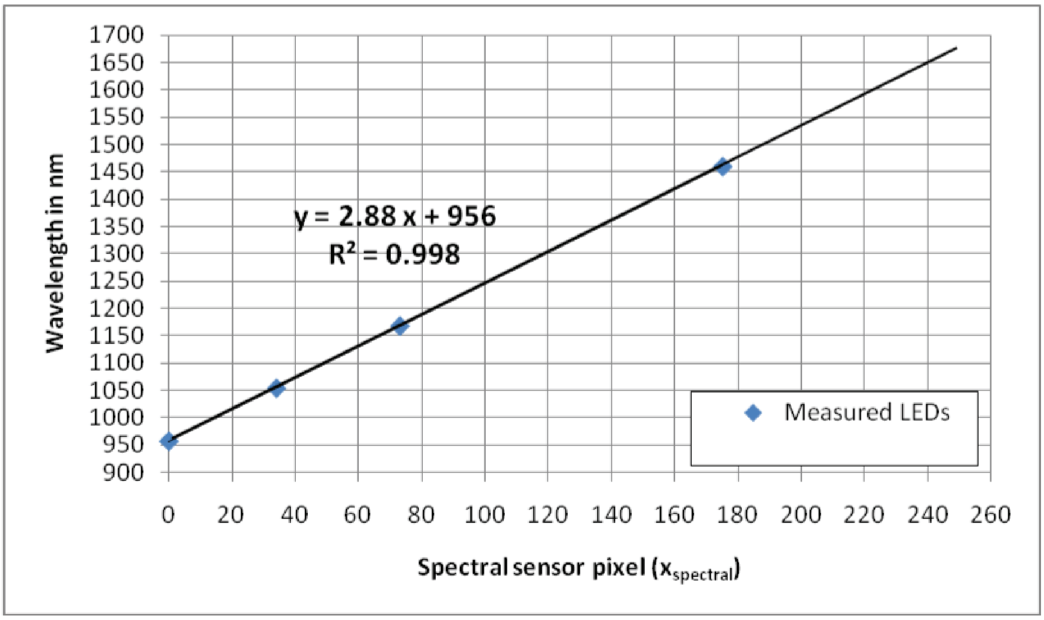

Figure 7: Wavelength/Sensor pixel calibration function of the Helios Core System

A linear regression curve with a determination coefficient of 0.998 based on 4 values was calculated:

$$Wavelength = (956 + 2.88 * x_{spectral}) \, nm \qquad | \; x_{spectral}: \text{position of spectral pixel}$$

Based on this equation the spectral range of 956 nm up to 1679 nm of the sensor system can be calculated. The spectral step size limited by the count of 252 spectral pixels is 2.87 nm / pixel.

2.3 Spectral resolution

The spectral resolution of the Helios Core is specified by EVK less than 9 nm FWHM using the sensor system with the 30 µm entry slit. To achieve a high light sensitivity of the system for online measurements our configuration was equipped with a larger slit width of 100 µm. To measure the resolution of this special spectrograph configuration a laser with a narrowband peak wavelength of 1454 nm was measured by the Helios Core as well as by the Tec5 spectroscope for monitoring.

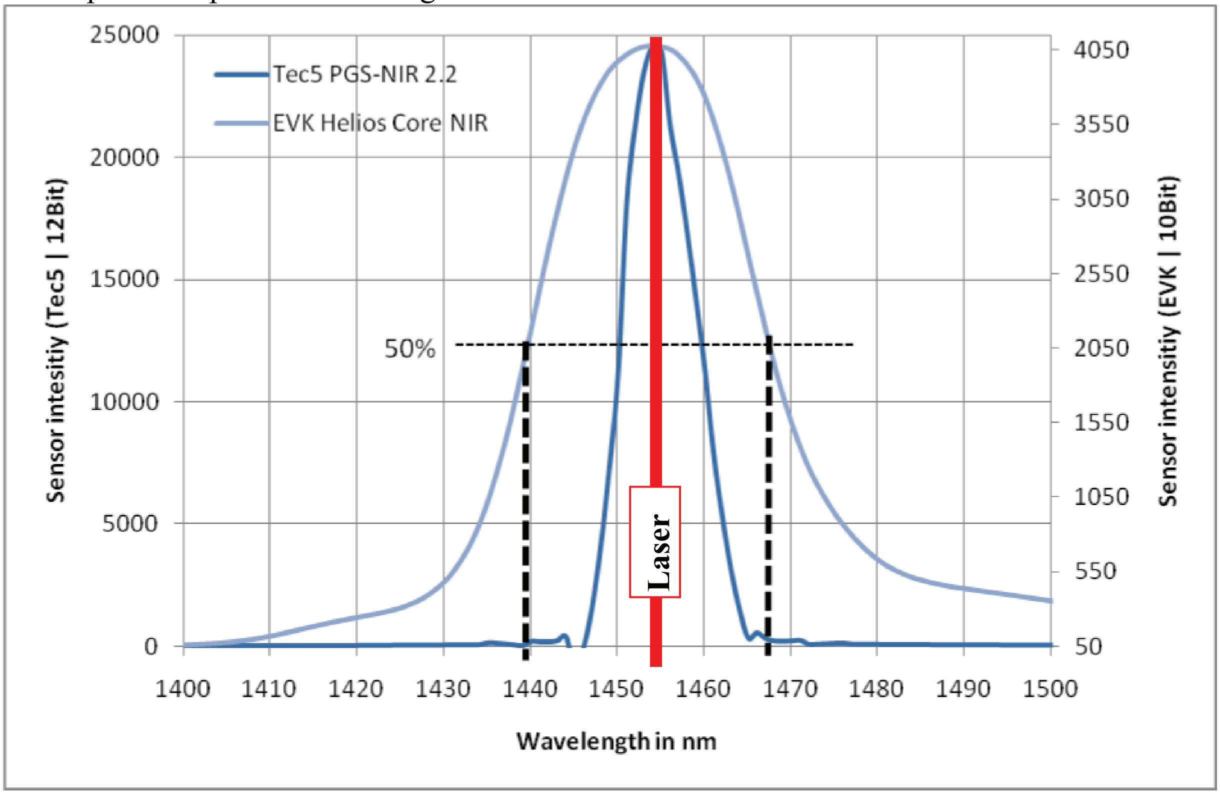

Figure 8: measurement of the spectral resolution of the Helios Core system by scanning the spectral illumination-width of a Laserdiode (Laser-peak at 1454 nm)

The measured spectral intensity of the laser-diode using the Helios Core with a spectrograph entry slit of 100 µm is shown in Figure 8. Based on this the spectral resolution of the Helios Core system was calculated:

$$\text{Spectral resolution}_{\text{Helios Core}} = 28 \text{ nm (FWHM @ 100 µm slit)}$$

2.4 Width of scan line

The self defined boundary condition for online usability of the measuring system was to be able to measure objects at the ground plate with a movement speed up to 1 m/s without losing spatial information. To determine the required frame rate of the system the width of the scan line on ground level has to be known. Therefore a black to white pattern with high contrast has been moved orthogonal to the sensor scan line. The movement was realized by a stepper motor which offers a high accuracy of the moved linear path correlated with the spectral reflectance data of the sensor.

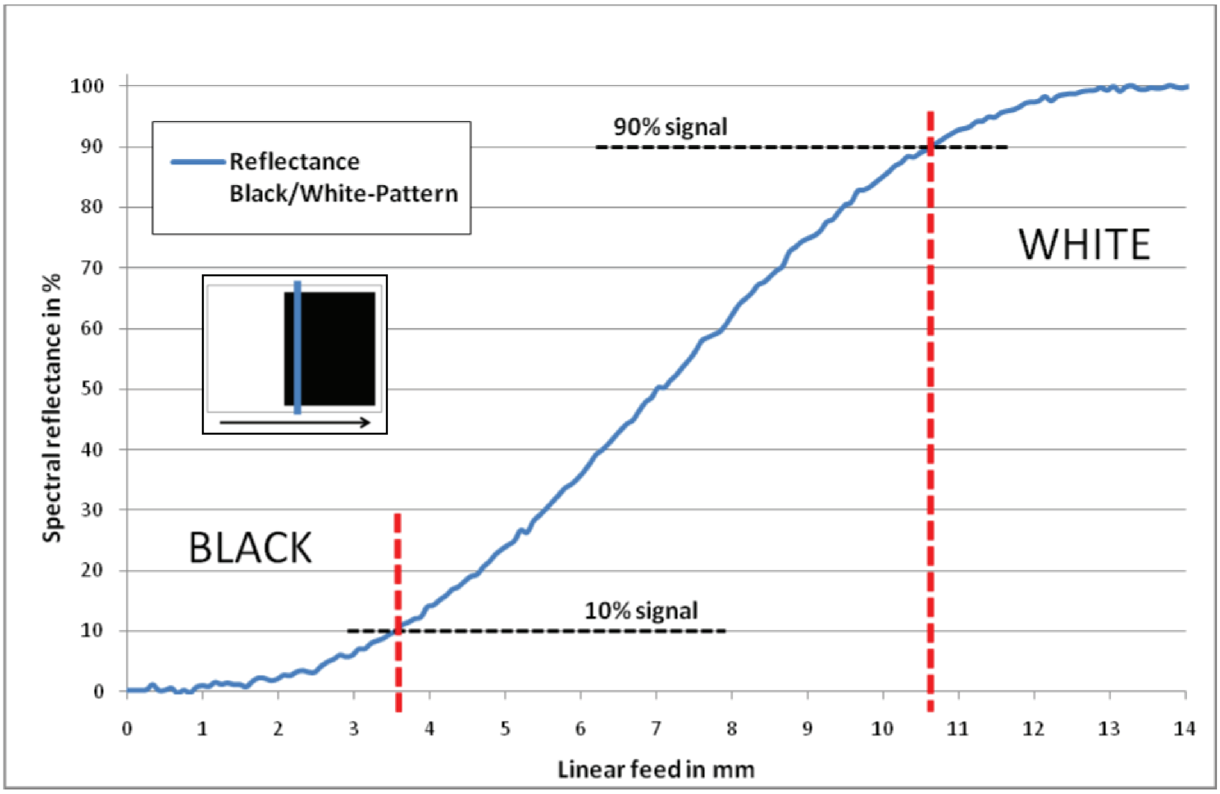

Figure 9: Gradient of reflectance intensity of a single sensor pixel passing a black to white step orthogonal to the scan line (object on system ground level)

In Figure 9 the normalized reflectance intensity of the black-white pattern is shown. When the black area moves out of the scan line the intensity increases until the whole scan line width is completely above the white area. Between the minimum and maximum of the reflectance intensity the scan line has an overlap to the black and white area. The moved distance until the reflectance intensity increases from 10% up to 90% is defines as the effective scan line width (Burke 1996).

$$\text{Scan line with}_{\text{ground level}} = 7 \text{ mm}$$

The corresponding frame rate of measuring objects with a relative movement speed Δv of 1m/s with a scan line width $x_{scanline}$ of 7 mm is:

$$frame\ rate_{min} = \frac{\Delta v}{x_{scanline}}$$

$$frame\ rate_{min} = 143\ s^{-1}$$

Based on this calculation the frame rates of the spectral imaging system for the following measurements are preset to 150 frames / second.

2.5 Signal to noise level

The noise level was measured by using a reference object at a typical sensor signal level of 50% and at a frame rate of 150 fs^{-1}. The noise standard deviation was calculated of 100 frames for each pixel of the CCD sensor.

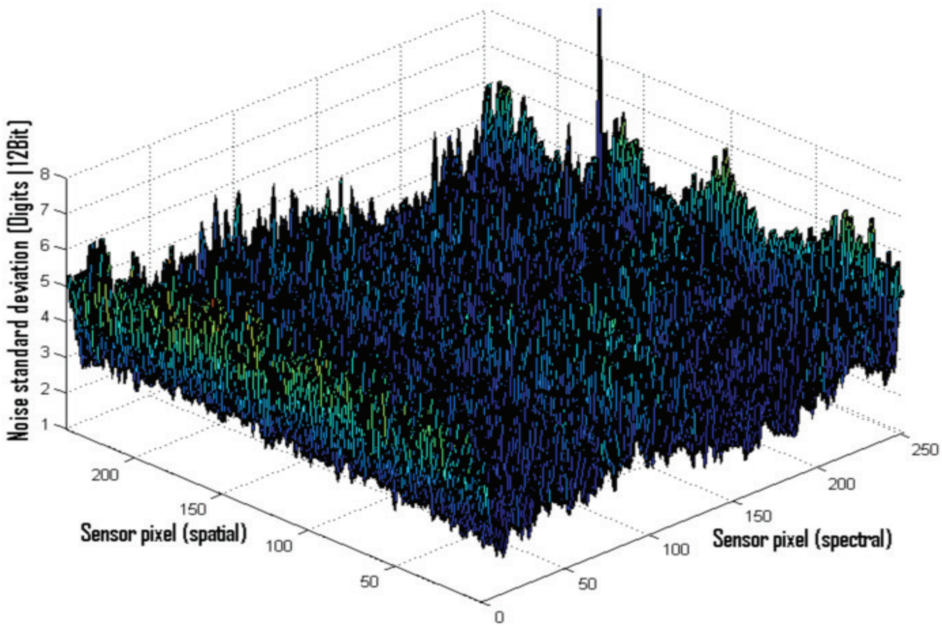

Figure 10: Standard deviation of pixel noise (sample rate 150 fs^{-1}, signal intensity average 50 % of 12 Bit)

Based on this data the mean value of the noise standard deviation level was calculated:

$$\sigma_{noise} = \frac{1}{n}\sum_{i=1}^{n} \sigma_{noice,i} \qquad | \quad n = count\ of\ pixel$$

$$\sigma_{noise} = 3.47\ Digits$$

The light intensity of the illumination (2 x 65 W halogen spot light) has been measured at 9 different heights from 40 cm down to 0 cm in reference to the ground plate. As reference object a wooden slat was chosen because of its nearly similar reflectance characteristic to a dry leaf. The aperture was adjusted that the maximum intensity all over the measurement height and width is close below the saturation of the sensor (4095 Digits). Exemplified the reflectance intensity at the wavelength of 1.1 µm is shown in the following figure.

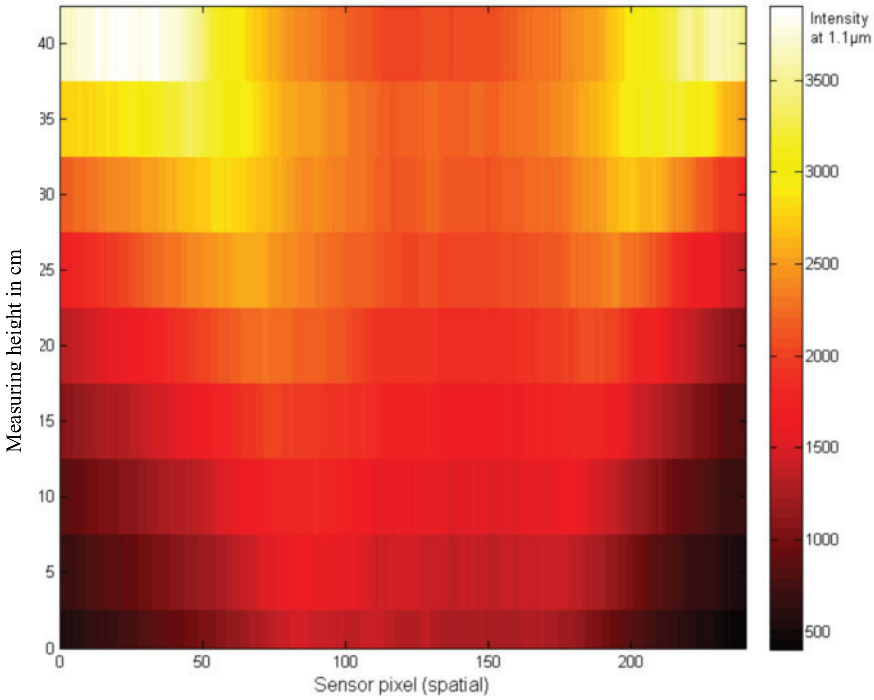

Figure 11: Reflectance intensity of a standardized object in dependence of the object height above system ground level and its spatial location along the scan line (intensity measured at 1.1 µm wavelength, intensity maximum 12 Bit = 4095 Digit)

Based on this signal intensity array of the 2D measurement space the minimum and maximum signal to noise ratio can be calculated exemplary for the wavelength of 1.1 µm:

$$SNR_{i|dB} = 20 \log \left(\frac{S_i}{N_i} \right)$$

$$SNR_{min|dB} \ @1.1\mu m = 43.17$$
$$SNR_{max|dB} \ @1.1\mu m = 61.23$$

This calculation must be performed to each spectral pixel of the whole spectral range of the sensor system to get a 3D matrix of the signal to noise ratio in dependency to the axe of the scan line, the height and wavelength.

2.6 Spatial resolution

To get information about the spatial resolution of the sensor system in direction of the scan line black lines with different thickness were measured static at the ground level of the sensor plate. The count of spatial pixels of the CCD chip is 240. Thus a theoretic spatial resolution is given by:

$$d_{theoretic} = \frac{length_{scan\ line}}{pixel_{spatial}}$$

$$d_{theoretic} = 2{,}92\ mm$$

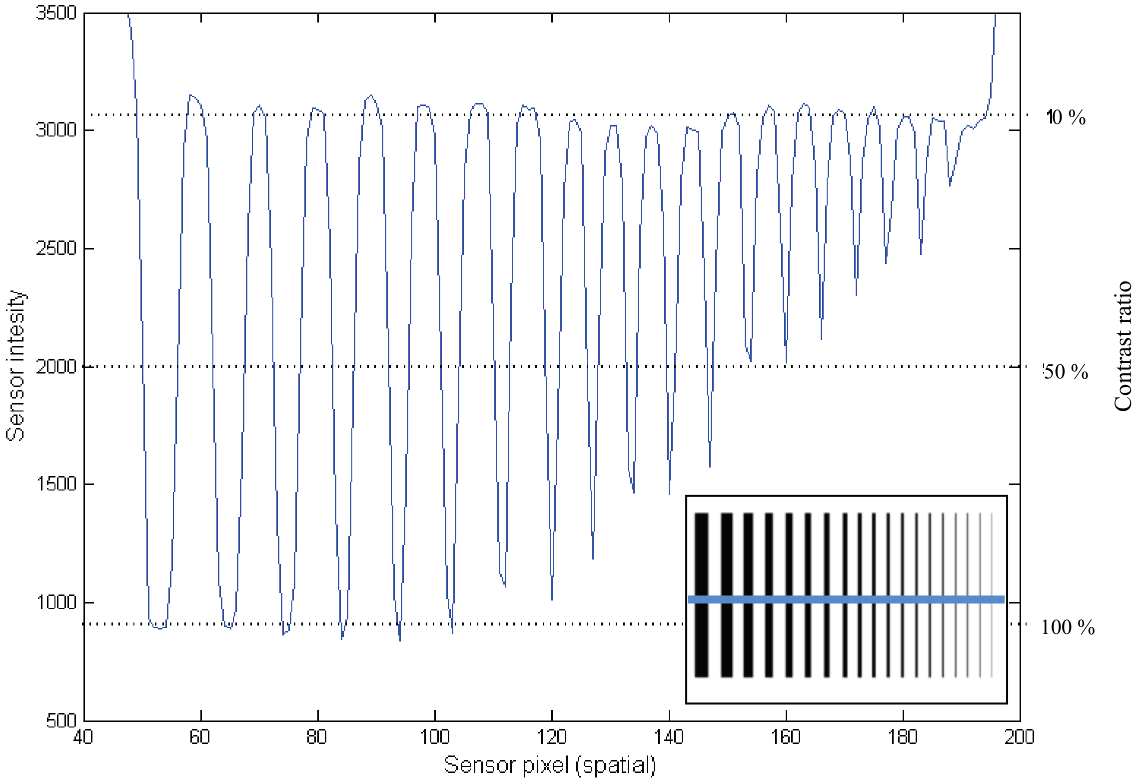

Figure 12: Measurement of the spatial resolution by analyzing the maximum contrast ratio of black lines on white ground (reflectance wavelength of 1.1 µm; line thickness from 12.5 mm down to 0.6 mm)

The measured data are correlating with the theoretic calculation and approve an optimal focusing of the optic. The first six lines (from left to right) have a thickness from 12.5 mm down to 5.7 mm and the measured reflectance contract of the sensor is 100 %. In case of Line width < 2 x $d_{theoretic}$ it is not guaranteed, that the sensor pixel is overlapped totally with the black line. Thus the contrast ratio goes down at structures smaller than 5.84 mm and fades below 50 % at lines smaller than 2.7 mm.

2.7 First spectral plant measurement

To get a first practical experience of the potential of the sensor data measured by the spectral imaging system a courgette plant with a maximum height of 30 cm was measured with the test setup. The illumination was done by two 65 W halogen spots, the measuring frame rate for the movement speed of 1 m/s was set to 150 s^{-1} and is consequently equivalent to the experiments of the system characterization.

Figure 13 shows a courgette plant having leafs with different heights and conditions.

Figure 13: RGB-picture of a courgette plant

The following figures show the results of the reflectance measurement performed by the Helios Core system. Comparing the first two figures the differences of the reflectance intensity at 1.0 µm and 1.46 µm are pointed out. In opposite to the plant surface the reflectance intensity of the soil at both wavebands is nearly constant at 20 % of signal range. The reflectance intensity of the plant surface is between 20 % - 44 % and correlates at the waveband of 1.0 µm directly to the height. At the waveband of 1.46 µm the reflectance intensity is strongly influenced by moisture.

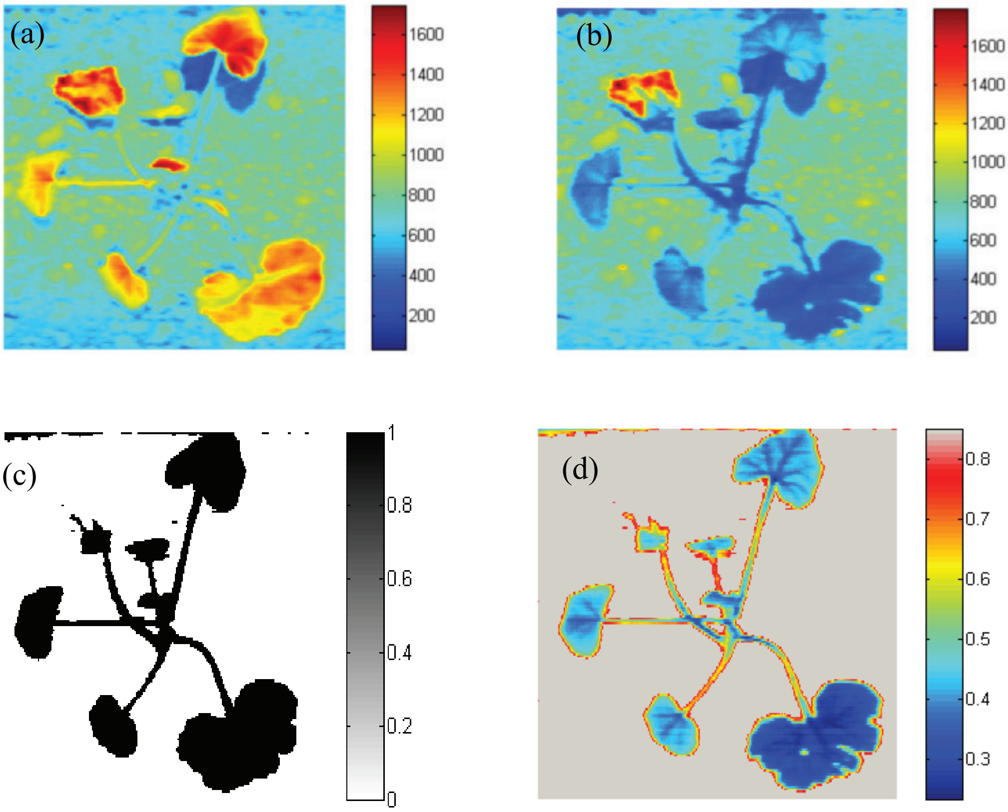

Figure 14: Reflectance intensity of the courgette plant at 1.0 µm (top left); reflectance intensity of the courgette plant at 1.46 µm (top right); image processed binary picture of plant

structures (bottom left); determined moisture distribution of the courgette plant calculated with the water index (bottom right)

Using image processing tools a binary picture is generated based on the spectral characteristic data (Figure 14c). Masked with the binary picture the result of the calculated water index was shown on Figure 14d. The boundary pixels of the plant structure show the influence of the spatial sensor resolution by averaging the reflectance of close environment e.g. soil. Anyway small structures and differences of the water index can be detected as seen at the upper and lower right leaf of Figure 14d.

4. CONCLUSIONS AND OUTLOOK

The influence of water to the reflectance intensity of leafs and soil has been shown and a basic water index has been established. Using sponges with different moisture levels a correlation between the water index based on reflectance data and the water content of the sponges has been shown.
Experimental methods ware performed to characterize the spectral imaging sensor. The illumination of 130 W halogen spot light is sufficient to allow high scan rates ups to 150 f/s with a lens aperture of 5.6 to get a sufficient depth of sharpness. Related to the object height up to 40 cm the illumination distribution at the scan line has been measured, the range of SNR has been calculated. Also the spatial resolution and the width of the scan line at ground level were measured.
The analyses of the Helios Core NIR spectral imaging system offers a high linearity of its spectral pixel to wavelength in the working range between 956 nm and 1682 nm. The spectral resolution of 28 nm (FMHW) is clearly sufficient for moisture measurements considering the width of the water absorbance band of water.
A measurement of a whole plant has been performed. This visualized data shows a good result of the calculated water index based on the spectral reflectance.

To realize a high correlation to the plant moisture further research of plant characteristics and environmental influences e.g. illumination disturbances caused by ambient light are necessary. Anyway a high usability of the NIR spectral imaging for visualizing plant moisture is given.

Acknowledgement
This work is supported by the Federal Ministry of Food, Agriculture and Consumer Protection BMELV (Germany).

5. REFERENCES

Burke, M. W.: Image Acquisition, vol. 1 of Handbook of machine vision engineering, Chapman & Hall, London, 1996
Dicke, D.: Lenkung der Teilschlagspezifischen Unkrautkontrollverfahren unter Berücksichtigung der Populationsdynamik von Unkräutern mit computergestützten Modellen. Dissertation, Universität Bonn, 2005.

Groell, K., Graeff, S., Claupein, W.: "Use of leaf-based sensor technologies to assess the effects of various plant diseases on wheat growth and development"; Proceedings of CIGR EurAgEng/ VDI-MEG, 2006.

Hellebrand, H.J., Dammer, K.H., Beuche, H., Herppich, W.B., Flath, W.: "Infrarotbildverfahren im Pflanzenschutz", Landtechnik 60, S. 142-143, 2005.

Larsolle, A., Muhammed, H.: "Mesuring crop status using multivariate analysis of hyperspectral field reflectance with application to disease severity and plant density Precision Agric (2007)8.

Ruckelshausen, A., Biber, P., Dorna, M., Gremmes, H., Klose, R., Linz, A., Rahe, F., Resch, R., Thiel, M., Trautz, D. and Weiss, U.; BoniRob – an autonomous field robot platform for individual plant phenotyping, Proceedings of the 7th European Conference on Precision Agriculture, Wageningen Academic Publishers, 2009, pp. 841-847.

Smolyar, N.: Bildgebende Spektroskopie an Pflanzenblättern. Dissertation, Universität Heidelberg, 2003.Thomas, E.: „Feldversuchswesen", Verlag Eugen Ulmer Stuttgart, ISBN 3-5252-8319-4 (UTB), 2006.

Walther, U., Flath, K., Moll, E., Prochnow, J., Sachs, E.: „Methodische Anleitung zur Bewertung der partiellen Resistenz von Sorten bzw. Linien unter Berücksichtigung epidemiologischer Aspekte", Mitt. Biol. Bundesanst. Land- Forstwirtsch. 374, 2000.